PURPOSE-LED PUBLISHING™

PAPER • OPEN ACCESS

Investigation of the effect of prescribed coupled motions on the power production of a floating offshore wind turbine

View the article online for updates and enhancements.

ECS UNITED

The Electrochemical Society
Advancing solid state & electrochemical science & technology

247th ECS Meeting
Montréal, Canada
May 18-22, 2025
Palais des Congrès de Montréal

Abstracts due December 6th

Showcase your science!

Investigation of the effect of prescribed coupled motions on the power production of a floating offshore wind turbine

R Ramponi[1,2], R Amaral[2] and A Viré[2]

[1] Politecnico di Milano, Dipartimento di Scienze e Tecnologie Aerospaziali, B12, Via La Masa 34, Milano, Italy

[2] Delft University of Technology, Faculty of Aerospace Engineering, Kluyverweg 1, 2629 HS Delft, Netherlands

E-mail: `riccardo1.ramponi@mail.polimi.it`

Abstract. Floating offshore wind turbines are subjected to platform motions that modify the local velocity experienced by the rotor. This work analyzes how variations in the platform motions affect the aerodynamic power of a floating wind turbine. Idealized wind conditions and rigid wind turbine are considered. The platform motions are prescribed by the user and the coupled motions considered are pitch-surge, pitch-yaw and surge-yaw. The main novelties of the work consist in the fact that multiple motions are prescribed simultaneously, including yaw, and that the prescribed motions present a difference in phase. In absence of wind turbine controller, the pitch-surge coupling shows significant increase in average power production with respect to fixed conditions when either the amplitude or frequency are increased. This gain is maximum when surge and pitch are in phase, and is almost zero in phase opposition. The presence of the controller reverses the behavior and introduces a loss in average power along with increasing amplitudes. Phase shift analysis is particularly interesting in the surge and pitch cases: the controller introduces an upper limit in power, and phase opposition is now desirable. The yaw degree of freedom is shown to be of secondary importance in every condition.

1. Introduction

Europe is one of the most virtuous areas in the world in the challenge to switch to a greener production of energy. According to Wind Europe [1], in 2022, Europe's wind farms covered 17% of the electricity demand in the European Union (EU-27) and the United Kingdom, making wind energy the most widespread alternative to fossil fuels and gas.

Wind turbines placed offshore offer technical advantages to increase power production. They are subjected to steadier wind conditions, as wind turbulence is reduced offshore due to lower surface roughness of the sea compared to onshore environments. Also, noise constraints are less strict outside inhabited regions. Wind Europe data from 2022 [1] also show that the capacity factor (CP) of new offshore wind farms ranges between 42% and 55%, against 30-35% for onshore machines. For offshore turbines with fixed foundations, costs, material use, and complex maintainability become a challenge at increasing water depths. This can be alleviated with floating turbines, where the turbine is mounted on a floating support structure held by anchors and mooring lines, hence offering potential for reduced costs and material use far-offshore and in deeper waters [2]. However, these floating turbines are subjected to platform

motions which inevitably change the local flow behaviour at the rotor. Several studies have investigated single degree of freedom (DOF) motions, mainly pitch [3, 4] and surge [5, 6]. A few have considered the pitch and surge DOFs applied simultaneously [7, 8]. The present article adds to this body of literature by providing a more in-depth investigation of the effects of prescribed coupled motions on the power production of a 15MW turbine [9], introducing phase shift among the motions and including less common DOFs in the analysis, such as yaw.

2. Methodology
Prescribed motions in two degrees of freedom are imposed on the WINDCRETE OpenFAST model of the IEA 15MW reference wind turbine [9, 10]. The turbine's main features are summarized in Table 1. Results are obtained with the open-source software OpenFAST v3.1.

Table 1. Characteristics of the IEA 15 MW reference turbine [9].

Parameter	Units	Value	Parameter	Units	Value
Power rating	MW	15	Rotor diameter	m	240
Turbine class	-	1B	Hub height	m	150
Number of blades	-	3	Maximum tip speed	m/s	95
Cut-in wind speed	m/s	3	Rated tip speed ratio	-	9.0
Rated wind speed	m/s	10.59	Minimum rotor speed	RPM	5.0
Cut-out wind speed	m/s	25	Maximum rotor speed	RPM	7.56

First, the initial turbine offset is computed by simulating the complete floating wind turbine (including hydrodynamics and mooring system) under rated wind conditions (wind speed of 10.59 m/s). The aerodynamic analysis uses the blade element momentum (BEM) theory, with steady aerodynamic models for blade airfoil and the use of the uncoupled BEM solution technique without an additional skewed-wake correction [11]. Prandtl tip-losses, hub-losses, and tangential induction factor are included in the analysis. Furthermore, drag terms are included in both the axial-induction and the tangential-induction calculations. Sea-state is generated with a JONSWAP spectrum [12], with a 70-minute long simulation. The wave period is $T = 9.01$s, the significant wave height is $H_s = 2.15$m, and the peak-shape parameter is $\gamma = 3.3$, which are realistic values. In order for the initial conditions to be as realistic as possible, aero-elasticity is included in the analysis, and the controller is activated. The controller is a COREWIND adaptation of ROSCO for floating wind turbines [13]. The active proportional integral (PI) controller operates in three regions [9]. Notably, the turbine is torque-regulated in the above-rated regime, resulting in constant power curve in steady conditions. All the platform degrees of freedom are active in order to find their values in steady conditions. Surge and sway values are zeroed as their initial condition is only a translation in the water plane, which does not affect the way wind interacts with the rotor.

Once the initial offset is found, OpenFAST simulations are further run for prescribed motions of the turbine, in order to perform a parametric analysis. Thus, the mooring lines and hydrodynamics sub-modules are deactivated. The wind turbine can move along the degrees of freedom of the prescribed motions, starting from the computed offset, with the goal to isolate the effect of the prescribed motions on the aerodynamics of the rotor. Additionally, the wind turbine is modeled as a rigid structure. The wind is uniform both in the horizontal and in the vertical direction, steady and with rated speed (10.59 m/s); no turbulence is added. This is of course somewhat unrealistic. However, this enables us to assess the fundamental

(and isolated) consequences of coupled degrees-of-freedom on the wind turbine performance. A follow-up study will consider inflow turbulence, and will be able to further assess its influence compared to the present results. Tower influence is neglected both in the wind model and in the aerodynamic loads calculation, since it does not significantly impact the average thrust force [14]. Two scenarios are considered: the first one does not include the controller and is useful for a pure aerodynamic investigation, whilst the second one includes the controller and aims at more realistic results. They will be referred as "scenario 1" and "scenario 2", respectively.
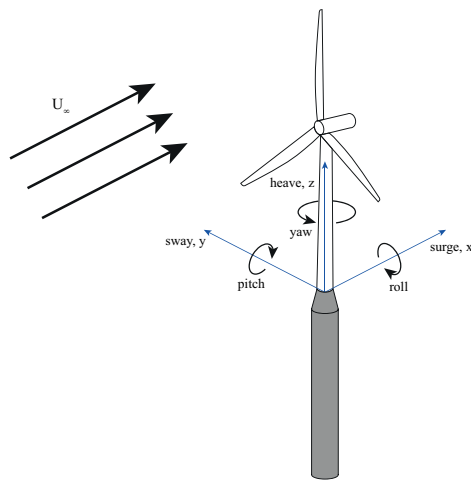
Figure 1. Wind turbine platform's degrees of freedom.

The wind turbine DOFs are defined according to Fig. 1. The imposed motions are prescribed through the ExtPtfm module of OpenFAST, which reduces the external platform to a mass-spring-damper system [15]. The motions of two arbitrary DOFs, x_1 and x_2, are imposed as

$$x_1(t) = A_1 \sin(2\pi f_1 t + \phi), \tag{1}$$
$$x_2(t) = A_2 \sin(2\pi f_2 t), \tag{2}$$

where $A_{1,2}$ and $f_{1,2}$ indicate the amplitudes and frequencies of the two motions prescribed, respectively, and ϕ denotes the phase shift between them. Three different combinations of motion are considered: surge-pitch, pitch-yaw, and surge-yaw. The values of frequencies and amplitudes considered in this work are indicated in Table 2. Small values of frequencies and amplitudes correspond to normal working conditions, while large values correspond to extreme conditions [16]. The natural frequencies of surge, yaw and pitch [16] are included in the test matrix.

Table 2. Values of the frequencies and amplitudes of motion considered in this work.

Motion	Frequencies	Amplitudes
Surge	{0.01221, 0.02441, 0.03052, 0.05, 0.07, 0.09155} Hz	{2, 4, 6, 8, 10} m
Pitch	{0.01221, 0.02441, 0.03052, 0.05, 0.07, 0.09155} Hz	{1, 2, 3, 4, 5} °
Yaw	{0.01221, 0.02441, 0.03052, 0.05, 0.07, 0.09155} Hz	{1, 2.75, 4.5, 6.25, 8} °

A sensitivity analysis was performed to identify a suitable time step value for the simulations. Surge-pitch motions with the lowest and the highest value of frequency were prescribed for this

analysis. It was found that the results in average power only differ by 0.05 % between cases with
`DT=0.01s` and `DT=0.1s`, hence the latter was chosen in this analysis. The transient time is set to
100s for scenario 1 and 400s for scenario 2, based on the time histories of the initial simulations.
After this transient, the simulations are run for at least 300s or 15 times the maximum period
among the prescribed frequencies. This value of number of periods was chosen by comparing the
obtained results to simulations where a maximum time of 50 periods were considered, leading to
only 0.1 % difference in average power. The mean power is calculated by taking a Fast Fourier
transform (FFT) of the time evolution of the power signal and considering the zero-frequency
value. This is because the interaction of two motions with different frequencies, and a phase
shift, makes it hard to identify a common time period for performing averaging in the time
domain. The power signal is windowed in time with a Hann window [17], before being processed
with the FFT. The average value of power is used as key parameter to analyze the impact of
the motions on the turbine performance.

## 3. Results without controller

3.1. Time histories

The first set of results has been achieved without including the controller. The pitch-surge
coupling has been investigated first in time domain. Figure 2 shows that, for matching prescribed
frequencies, the peaks in aerodynamic power correspond to the neutral position during forward
motion, i.e. when the turbine is pitching and surging towards the wind. In this position, the
surge and pitch motions achieve the highest velocity of motion. By contrast, the smallest power
is retrieved during backward motion. Note that, according to notation, pitch and surge motions
are both negative when facing the incoming wind. The time histories are more complex when
the frequencies of the prescribed motions do not match, as shown by Fig. 3. In that case, the
fastest motion determines the position of the local maxima and minima in power production,
whilst the slowest motion adds a second fluctuation. Note that the second sub-chart is presented
in terms of equivalent velocities at hub height, thus introducing comparative quantities among
the considered DOFs. Surge equivalent velocity is the same as platform surge velocity, since the
motion is a translation. Pitch equivalent velocity is defined as

$$\tilde{v}_{pitch} = d_{pitch} \cdot \omega_{pitch}, \qquad (3)$$

where d is the lever arm of the pitch motion, i.e. the distance from the rotor hub to the pitch
center of rotation which is the tower bottom. Increasing fluctuations in aerodynamic power are
observed for increasing prescribed amplitudes of pitch and surge, as also shown by Fig. 4 for
varying surge amplitudes. By contrast, little fluctuations in power are obtained when varying
yaw amplitudes, as illustrated by Fig. 5 for a prescribed pitch-yaw motion. Note that results
under surge-yaw motions are consistently similar to those obtained under pitch-yaw motions,
and are therefore omitted in this paper.

3.2. Parametric analysis

Parametric analyses are performed for both pitch-surge and pitch-yaw couplings, whereby the
effect of varying one degree of freedom (whilst keeping the other one fixed) is quantified in
terms of average power. In this paper, the terms "mean power" and "average power" are used
interchangeably. The results shown in Figs. 6 and 7 indicate a general trend of increasing average
power along with increasing amplitude or frequency of the prescribed sinusoidal motions. The
non-monotonic pattern obtained during the pitch-surge motions in Fig. 6 also suggests a sort
of resonance that can enhance the power production when the frequency of surge and pitch
motions are a multiple of one another and no phase-shift is present. This is confirmed when
looking at the mean power under pitch-surge motions, for different values of the surge frequency
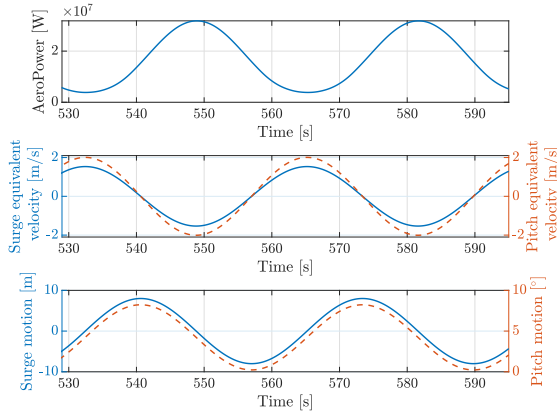
Figure 2. Time histories for $f_{pitch} = f_{surge} = 0.03052$ Hz, $A_{pitch} = 4°$, $A_{surge} = 8$ m. Top: aerodynamic power. Center: surge (blue) and pitch (red) equivalent velocities. Bottom: surge (blue) and pitch (red) motions.
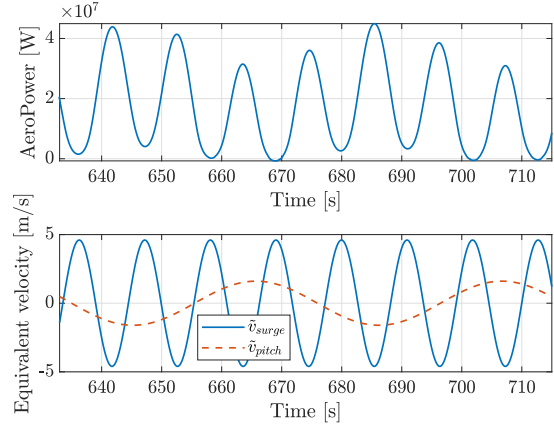
Figure 3. Time histories for $f_{pitch} = 0.02441$ Hz, $f_{surge} = 0.09155$ Hz, $A_{pitch} = 4°$, $A_{surge} = 8$ m. Top: aerodynamic power. Bottom: surge (blue) and pitch (red) equivalent velocities.
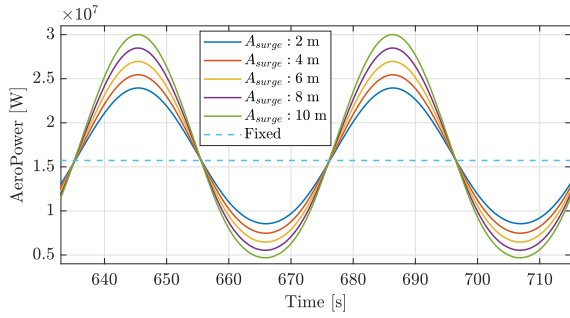
Figure 4. Time-domain response to pitch-surge motions with variable surge amplitudes, a fixed pitch amplitude of $A_{pitch} = 4°$, and $f_{pitch} = f_{surge} = 0.02441$ Hz (Scenario 1).
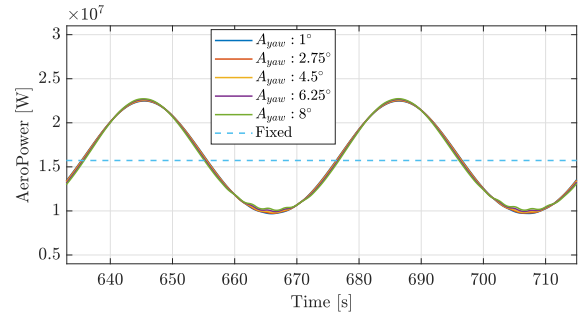
Figure 5. Time-domain response to pitch-yaw motions with variable yaw amplitudes, fixed pitch amplitude of $A_{pitch} = 4°$, and $f_{pitch} = f_{yaw} = 0.02441$ Hz (Scenario 1).

f_{surge} and fixed values of f_{pitch}, A_{pitch} and A_{surge} (Fig. 8). It is apparent that the mean power fluctuates when surge and pitch motions have equal frequencies. This effect is also spread to integer multiples of the assigned frequency, although with decreasing impact. The effect can be explained as follows. Under constant and uniform wind speed, the aerodynamic power is defined as

$$P = \frac{1}{2}\rho C_P A v_{rotor}^3. \tag{4}$$

Without any controller, and assuming small pitch angles, the only variation in the velocity at the rotor is due to the platform motion. The local velocity at the rotor, v_{rotor}, is thus defined as

$$v_{rotor} = v_{wind} + \tilde{v}_{surge} + \tilde{v}_{pitch}, \tag{5}$$

where $\tilde{v}_{surge}$ and $\tilde{v}_{pitch}$ are the equivalent velocities at hub height due to, respectively, surge and pitch motions. In the process of averaging equation 4, v_{rotor} is the dominant term for small pitch angles, due to constant tower height, and small C_P and rotor area variation. Finally, cubic root
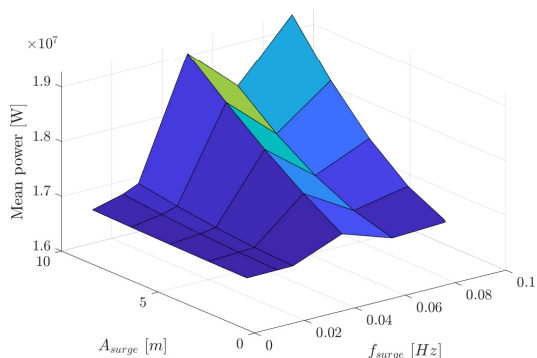
Figure 6. Mean power for pitch-surge motions with $f_{pitch} = 0.05$ Hz, $A_{pitch} = 4°$, and varying amplitudes and frequencies in surge.
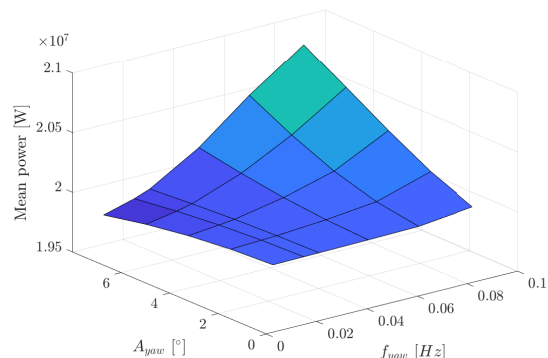
Figure 7. Mean power for pitch-yaw motions with $f_{pitch} = 0.09155$ Hz, $A_{pitch} = 5°$, and varying amplitudes and frequencies in yaw.

is taken to physically obtain a velocity: this way a cubic average velocity $\bar{v}_3$ is defined as

$$\bar{v}_3 = \left(\overline{v_{rotor}^3} \right)^{\frac{1}{3}}, \tag{6}$$

where the bar defines the averaging operator, here achieved with a FFT. The resonance effect is thus a consequence of the equal frequencies in the sinusoidal prescribed motions, combined with the non-linearity of v_{rotor} in the power definition ($P \propto v_{rotor}^3$).

The mean power and cubic average velocity show the same pattern, as demonstrated by comparing Figs. 8 and 9.

Figure 7 considers pitch-yaw coupling and shows how the variation of average power with yaw
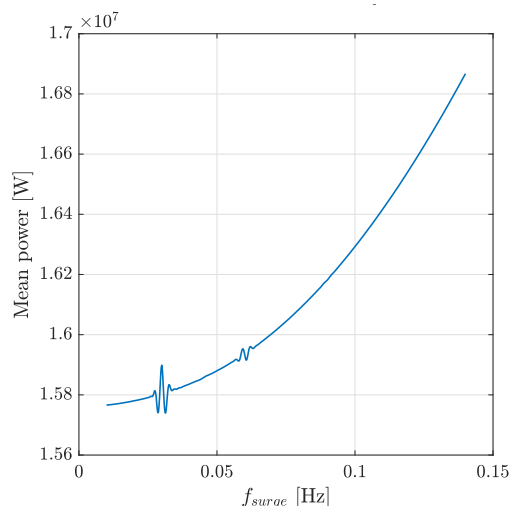
Figure 8. Resonance effect in pitch-surge motions: mean power as a function of surge frequency for $f_{pitch} = 0.03$ Hz, $A_{surge} = 4$ m, $A_{pitch} = 2°$.
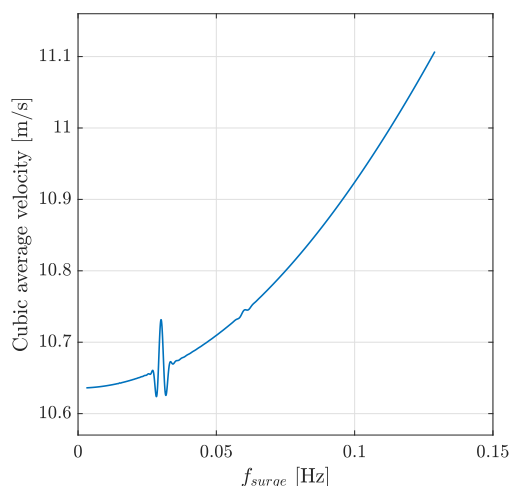
Figure 9. Resonance effect in pitch-surge motions: cubic average velocity as a function of surge frequency for $f_{pitch} = 0.03$ Hz, $A_{surge} = 4$ m, $A_{pitch} = 2°$.

amplitude is not always identical. Indeed, the power can decrease at increasing yaw amplitude,

when the yaw frequency is small enough. This happens, with different intensity, regardless of the pitch motion considered.

The phenomenon is observed because the yaw motion makes the rotor experience a velocity symmetric to the tower, thus the average velocity on the rotor is kept constant. Nevertheless, this velocity component is summed or subtracted from the wind velocity at the blades depending on the azimuthal position. The rotor velocity fluctuates in time and, since it acts on power with exponent three, it makes the average power grow for increasing amplitude or frequency in the yaw motion. This effect is counterbalanced by the velocity-rotor misalignment caused by the yaw motion, which induces a loss in power. On average, velocity-rotor misalignment only depends on the amplitude of yaw angle, not on the frequency. Consequently, when the yaw frequency is small, the gain in average power is smaller than the loss due to the misalignment. By contrast, when the yaw frequency is large, the gain in power is dominant over the misalignment.

3.3. Phase shift analysis

The influence of the phase shift is assessed in terms of average power. As described in the previous section, the average power is computed through a FFT. Figure 10 shows the percentage difference in mean power between a turbine under pitch-surge motion and a fixed turbine, for different values of phase shifts. In Fig. 10, each column represents the result of a whole simulation. It is apparent that, when the frequencies of surge and pitch are different (Fig. 10, left and centre), the phase shift between the motions has no influence in the mean power produced. This is due to the fact that, when the frequencies are not equal, the prescribed motions are already out of tune, and thus the resultant motion experienced by the rotor is not enhanced, or diminished, by a difference of phase between them. When the pitch and surge frequencies are equal, the difference in mean power between moving and fixed turbine is minimum when the motions are out-of-phase (Fig. 10, right).
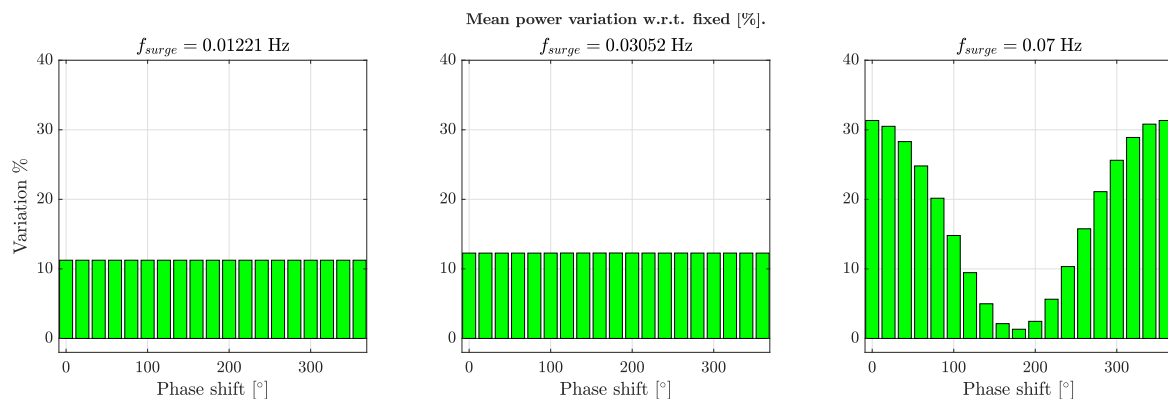
Figure 10. Variations in mean power under pitch-surge motion, compared to a fixed turbine, as a function of the phase shift for $f_{pitch} = 0.07$ Hz, $A_{pitch} = 4°, A_{surge} = 8$ m and three different values of surge frequency: $f_{surge} = 0.01221$ Hz (left), $f_{surge} = 0.03052$ Hz (centre), and $f_{surge} = 0.07$ Hz (right), scenario 1.

Although this investigation is presented for pitch-surge coupling only, the same observation holds for pitch-yaw and surge-yaw motions. Figure 11 highlights in more details the variations in average power production under surge-pitch motions with different phase shifts and motion frequencies: the values of pitch and surge amplitudes are chosen from the higher limit of the test matrix from Table 2 to demonstrate the phenomenon more plainly. Again, platform motions occurring in phase opposition yield poorer power performance with respect to in-phase motions, since the positive effect of one motion is negatively counterbalanced by the other, see v_{rotor} in
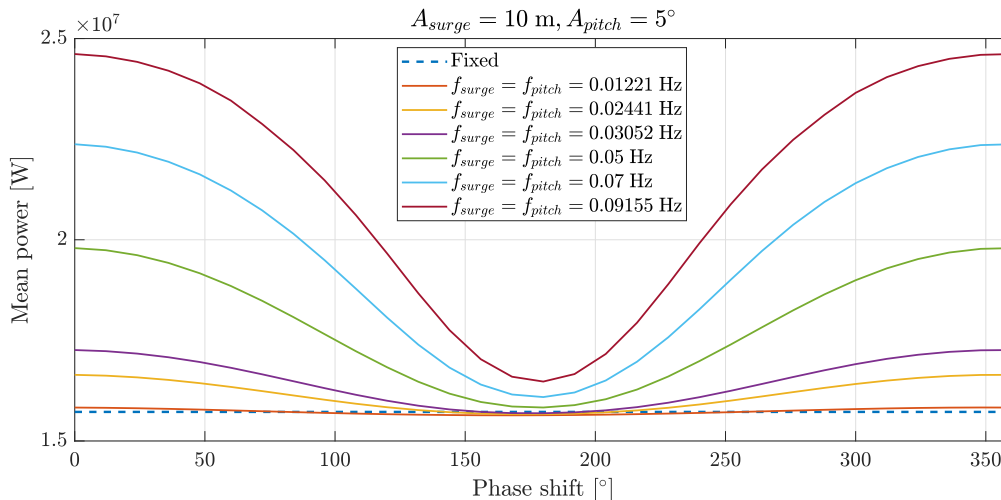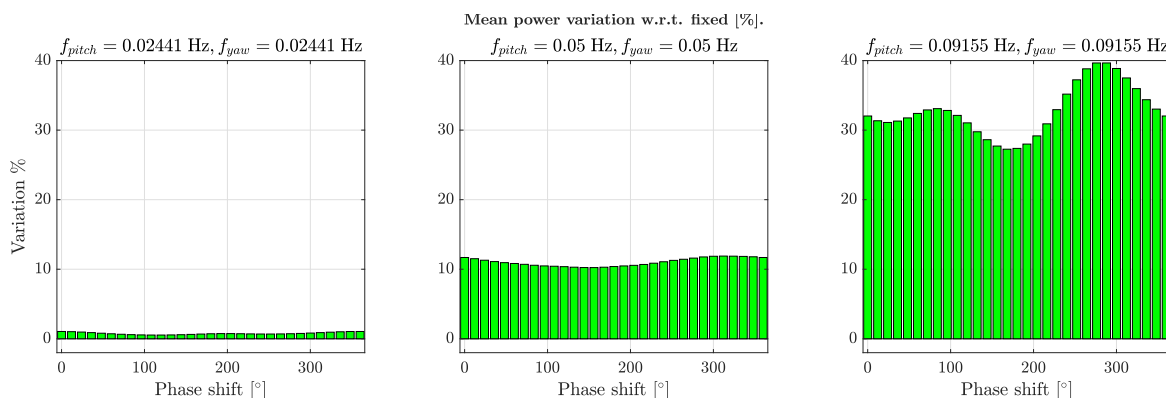
Figure 11. Variations in mean power under pitch-surge motion, as a function of the phase shift, for different values of $f_{surge} = f_{pitch}$, $A_{surge} = 10$ m and $A_{pitch} = 5°$ (Scenario 1).

Eq. (5). Notably, for the smallest values of frequency simulated, the mean power can be slightly inferior to the equivalent fixed turbine.

Although power loss looks restricted to minor relevance, it is important to consider that lower frequencies of motion occur and can thus be significant during the life cycle of the wind turbine. Also, the most likely amplitudes are normally below the one proposed in Fig. 11: in normal conditions the percentage of power loss, or gain, is thus drastically reduced.

Whilst the pitch-surge pattern of average power is symmetric along phase shift, with a 2π periodicity, this is not the case for the variations of mean power under pitch-yaw motion, as shown by Fig. 12. The behavior is unexpected: although initially supposed to be linked to
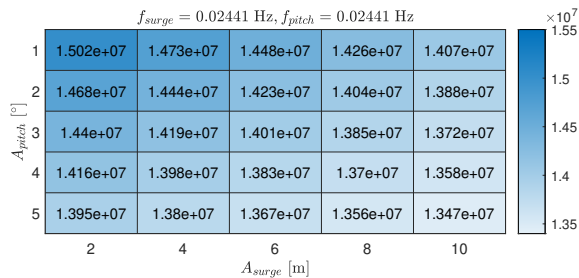

Figure 12. Variations in mean power under pitch-yaw motion, as a function of the phase shift, for $A_{pitch} = 5°$, $A_{yaw} = 8°$, and three values of pitch frequencies: $f_{pitch} = f_{yaw} = 0.02441$ Hz (left), $f_{pitch} = f_{yaw} = 0.05$ Hz (centre), $f_{pitch} = f_{yaw} = 0.09155$ Hz (right), scenario 1.

the asymmetric initial conditions, it can be shown to happen also if no offset is present. The hypothesis is that the described behavior is a consequence of the coupling of pitch and yaw: since the two DOFs introduce different rates of acceleration on different regions of the rotor, there will be different resultant accelerations depending on the phase shift. By contrast, the

surge-yaw coupling (not shown here) recovers symmetry along the phase shift.

The results for the coupled surge-pitch motions are of practical relevance, since the natural frequencies of each of the two DOFs can be observed in the other's spectrum in an aero-hydro-elastic simulation [18]. The results for pitch and yaw coupling are, instead, mainly theoretical.

4. Results with controller

Whilst the previous results show possible increase in mean power under coupled motions of the turbine, in the absence of controller, this is not the case when the controller is active. Indeed, due to the sinusoidal prescribed motion, the rotor effectively experiences wind velocities oscillating among below-rated and above-rated regimes. The controller design aims at maintaining torque constant in the above-rated regime, resulting in constant average power. Moreover, the controller effect on power in below-rated regime is negligible. Consequently, losses in mean power with respect to fixed conditions are observed from an averaged perspective. This observation is

Figure 13. Scenario 2: Mean power variations under pitch-surge motions for different motion amplitudes and fixed frequencies, i.e. $f_{pitch} = f_{surge} = 0.02441$ Hz.
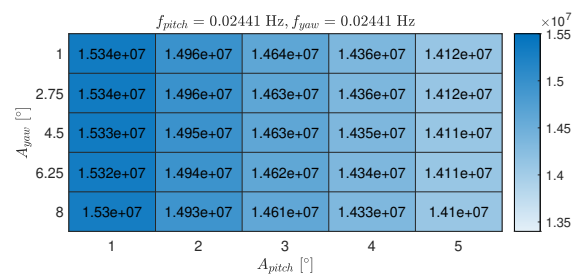

Figure 14. Scenario 2: Mean power variations under pitch-yaw motions for different motion amplitudes and fixed frequencies, i.e. $f_{pitch} = f_{yaw} = 0.02441$ Hz.

true for small values of prescribed frequencies, i.e. $f \le 0.4$ Hz. The probable reason is the inability of the controller to adapt to quicker variations in the state. Figures 13 and 14 show the discussed behavior for selected frequencies and amplitudes for pitch-surge and pitch-yaw motions, respectively. Prescribed frequencies are fixed and amplitudes are varying. Figure 14 shows that the mean power variations are mainly connected to pitch amplitude increase, thus again highlighting the secondary relevance of the yaw DOF. Figures 15 and 16 show that the dominance of pitch and surge over yaw is maintained also in scenario 2, which is more realistic as the turbine is controlled.

Phase shift analysis for controlled turbine detects significant patterns for pitch-surge coupling only. Whilst experiencing a larger platform-driven velocity was beneficial for the average power of the uncontrolled turbine, it is detrimental when the controller is active. For the controlled turbine, the larger the velocity oscillations, the larger the fluctuations between the controller regimes. This is a drawback in the below-rated region and does not allow power gain in the above-rated one, thus yielding an overall power loss which increases with the frequency of the platform motions.

5. Conclusions

This work analyzed the mean power produced by a wind turbine under the effect of prescribed 2-DOF motions. When the controller is disabled, it was shown that a prescribed pitch-surge motion leads to an increasing average power production when the amplitude and frequency of the motion increase. It was also found that, when both motions have the same frequency but are shifted with a certain phase angle, the potential gain in power can be reduced, and even be
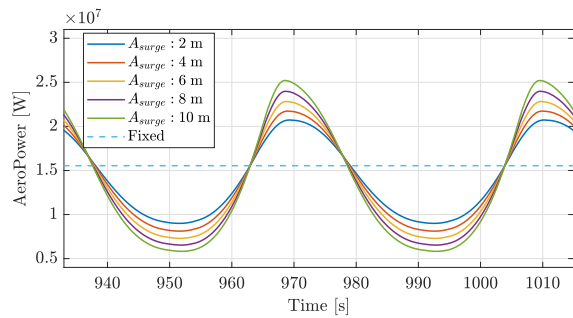
Figure 15. Time-domain response to pitch-surge motions with variable surge amplitudes, a fixed pitch amplitude of $A_{pitch} = 4°$, and $f_{pitch} = f_{surge} = 0.02441$ Hz (Scenario 2).
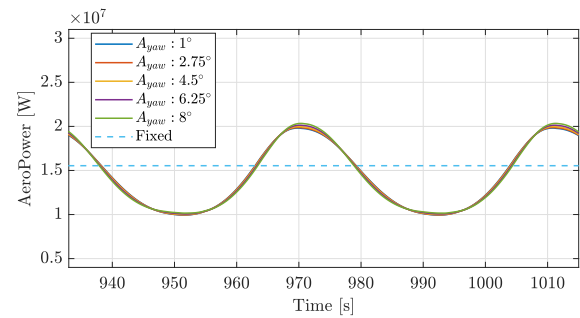
Figure 16. Time-domain response to pitch-yaw motions with variable yaw amplitudes, a fixed pitch amplitude of $A_{pitch} = 4°$, and $f_{pitch} = f_{yaw} = 0.02441$ Hz (Scenario 2).
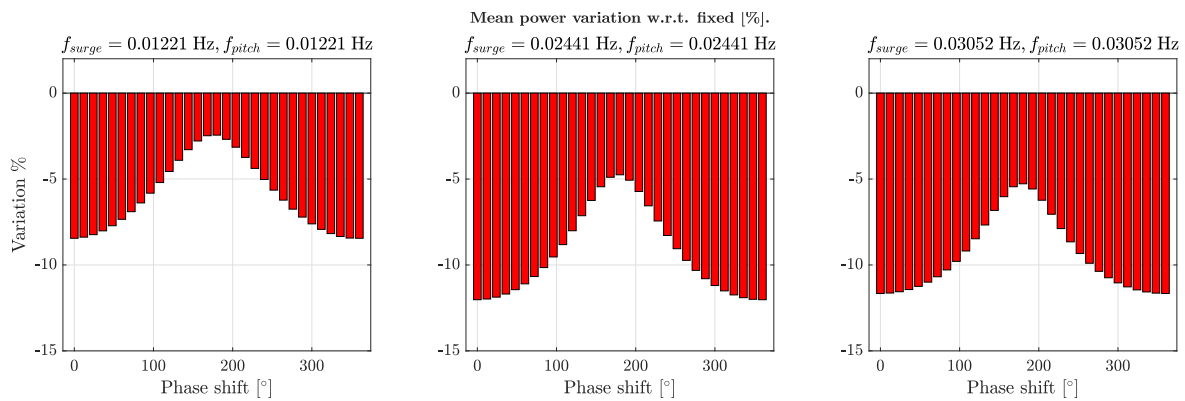
Figure 17. Phase shift analysis for matching frequencies of motions. Scenario 2, pitch-surge. Sub-plots show mean power decrease with respect to fixed turbine along with phase shift: the loss is maximum without phase shift and minimal when the motions are completely out of tune. $A_{pitch} = 5°$, $A_{surge} = 6$ m.

zero when the motions are out-of-phase.

When the controller is enabled, the power is limited in the above-rated regime. Therefore, the increase in platform motions leads to average power losses. When subjected to pitch-yaw and surge-yaw motions, it is found that the effect of pitch and surge motions are dominant over yaw. This is apparent both from the average power trend and from the amplitude of power oscillations in time domain. The main reason of this result is the alignment of pitch and surge motions with the incoming wind. Interestingly, when the controller is active, a phase shift between the motions can have a positive effect on the power produced, since the auto-compensating effect of motions in opposition of phase guarantees smaller translations between below- and above- rated regime. This work offers preliminary results on the effect of 2-DOFs prescribed motions. Although the work has significant simplifying assumptions, for example the absence of inflow turbulence, it offers some fundamental understanding of the interactions between coupled degrees of freedom and their influence on the power production of a floating wind turbine. This can be used as a baseline for future studies applying higher fidelity methods in the calculations of aerodynamic power with even more realistic conditions.

Acknowledgments

References

[1] WindEurope 2023 Wind energy in Europe: 2022 statistics and the outlook for 2023-2027
[2] Maalawi K Y 2020 *Design Optimization of Wind Energy Conversion Systems with Applications* (Rijeka: IntechOpen)
[3] Tran T T and Kim D H 2015 *Journal of Wind Engineering and Industrial Aerodynamics* **142** 65–81
[4] Jeon M, Lee S and Lee S 2014 *Renewable Energy* **65** 207–212
[5] Farrugia R, Sant T and Micallef D 2016 *Renewable Energy* **86** 770–784
[6] Mancini S, Boorsma K, Caboni M, Cormier M, Lutz T, Schito P and Zasso A 2020 *Wind Energy Science* **5** 1713–1730
[7] Chen Z, Wang X, Guo Y and Kang S 2021 *Renewable Energy* **163** 1849–1870
[8] Feng X, Lin Y, Zhang G, Li D, Liu H and Wang B 2021 *Journal of Marine Science and Engineering* **9**
[9] Gaertner E, Rinker J, Sethuraman L, Zahle F, Anderson B, Barter G, Abbas N, Meng F, Bortolotti P, Skrzypinski W, Scott G, Feil R, Bredmose H, Dykes K, Sheilds M, Allen C and Viselli A 2020 Definition of the IEA 15-megawatt offshore reference wind turbine Tech. rep. International Energy Agency
[10] Molins C, Trubat P and Mahfouz M Y 2020 UPC - WINDCRETE OpenFAST model 15MW FOWT - Grand Canary Island
[11] Ning S A 2014 *Wind Energy* **17** 1327–1345
[12] Hasselmann K and Olbers D 1973 *Ergänzung zur Deut. Hydrogr. Z., Reihe A (8)* **12** 1–95
[13] Abbas N J, Zalkind D S, Pao L and Wright A 2022 *Wind Energy Science* **7** 53–73
[14] Robertson A, Bergua R, Fontanella A and Jonkman J 2023
[15] Branlard E, Shields M, Anderson B, Damiani R, Wendt F, Jonkman J, Musial W and Foley B 2020 *Journal of Physics: Conference Series* **1452** 012033
[16] Mahfouz Y, Salari M, Vigara F, Hernandez S, Molins C, Trubat P, Bredmose H and Pegalajar-Jurado A 2020 D1.3. Public design and FAST models of the two 15MW floater-turbine concepts URL https://doi.org/10.5281/zenodo.4385727
[17] Oppenheim A V, Schafer R W and Buck J R 1999 *Discrete-Time Signal Processing* 2nd ed (Prentice-hall Englewood Cliffs)
[18] Ramachandran G K V, Robertson A, Jonkman J M and Masciola M D 2013